

THE PENNSYLVANIA STATE UNIVERSITY
SCHREYER HONORS COLLEGE

DEPARTMENT OF CHEMISTRY

Investigation of ZnSe Mn²⁺ Doped Nanoparticles Films for Use in Photocatalysis

YUYANG WANG
SPRING 2021

A thesis
submitted in partial fulfillment
of the requirements
for baccalaureate degrees
in Chemistry and Mathematics
with honors in Chemistry

Reviewed and approved* by the following:

John Asbury
Professor of Chemistry
Thesis Supervisor

Ben Lear
Associate Professor of Chemistry
Honors Adviser

* Electronic approvals are on file.

ABSTRACT

Photocatalysis shows the importance of creating green energy while taking advantages of the sun. Mn^{2+} doped ZnSe nanoparticles with long excited state lifetime can overcome the limit in photocatalysis, which brought up great interests. Then, Mn^{2+} doped ZnSe NPs were used to produce hydrogen. Mn^{2+} doped ZnSe NPs were made and deposited on film with NiO electrode, which was covered with 7 nm Al_2O_3 and different thickness of Pt. The film was put in 0.5 M ascorbic acid solution in 50:50 ethanol: water and excited with xenon lamp to produce H_2 . Over 23 hours, over 160 ppm of H_2 , about 0.05 μmol of H_2 , was made in the vial. H_2 was made using the structure developed in this project. The efficiency of producing H_2 using Mn^{2+} doped ZnSe NPs will be detected in the future.

TABLE OF CONTENTS

LIST OF FIGURES	iii
ACKNOWLEDGEMENTS	v
Chapter 1 Information.....	1
Sub-Chapter 1: Background Information and Significance.....	1
Sub-Chapter 2: Research Plans.....	3
Chapter 2 Result and Discussion	5
Sub-Chapter 1: Synthesis Part	5
Sub Chapter 2: Spin Coating NPs and Formatting the Structure.....	10
Chapter 3 Future Work	22

LIST OF FIGURES

Figure 1: Electron configurations of ZnSe and Mn ²⁺ doped ZnSe with spin-flip between ⁴ T ₁ and ⁶ A ₁ excited state.	3
Figure 2: Architecture of photocatalytic Al ₂ O ₃ coated ZnSe NPs doped with Mn ²⁺ ions to be explored in this project.....	4
Figure 3: Apparatus of synthesis of Mn ²⁺ doped ZnSe NPs.	5
Figure 4: Fluorescence color of Mn ²⁺ ZnSe NPs under the UV lamp (374 nm) made at Sept. 26, 2019.....	6
Figure 5: Emission data of eight samples of Mn ²⁺ ZnSe NPs made at different dates.....	7
Figure 6: Absorption data of eight samples of Mn ²⁺ ZnSe NPs made at different dates.	7
Figure 7: Time-resolved PL spectroscopy shows the long-excited state lifetime of Mn ²⁺ doped ZnSe NPs.	8
Figure 8: (A) Fluorescence of Mn ²⁺ doped ZnSe NPs films using (L) drop-casted and (R) spin-coated method under the UV lamp. (B) Absorption data of two films.	10
Figure 9: (A) Fluorescence of Mn ²⁺ doped ZnSe NPs film using spray-coated method under the UV lamp. (B) Absorption data of spray-coated film and spin-coated film with 20 layers.	10
Figure 10: Fluorescence of Mn ²⁺ doped ZnSe NPs with MPA under the UV lamp.....	12
Figure 11: Fluorescence of Mn ²⁺ doped ZnSe NPs with MPA and diheptyl MV ²⁺	12
Figure 12: Normalized absorption data of 8-layer Mn ²⁺ doped ZnSe NPs film with MPA before and after depositing diheptyl MV ²⁺	13
Figure 13: TA spectroscopy of Mn ²⁺ doped ZnSe NPs film with MPA with diheptyl MV ²⁺	14
Figure 14: Time-resolved PL spectroscopy of seven Mn ²⁺ doped ZnSe NPs films with MPA.	15
Figure 15: Four Mn ²⁺ doped ZnSe NPs films with MPA	16
Figure 16: Fluorescence of four Mn ²⁺ doped ZnSe NPs films with MPA with Al ₂ O ₃	17
Figure 17: Absorption data of four Mn ²⁺ doped ZnSe NPs films with MPA	18
Figure 18: Time-resolved PL spectroscopy of four Mn ²⁺ doped ZnSe NPs films with MPA with different thickness of Al ₂ O ₃ layer.	19
Figure 19: TA spectroscopy of sample 2 and 4 with hydrate MV ²⁺	20
Figure 20: Four Mn ²⁺ doped ZnSe NPs films with MPA and 7 nm Al ₂ O ₃	22

Figure 21: Fluorescence of four Mn ²⁺ doped ZnSe NPs films with MPA and 7 nm Al ₂ O ₃ with different thickness of Pt under the UV lamp.	23
Figure 22: Mn ²⁺ doped ZnSe NPs with MPA and 7 nm ALD and 1.5 nm Pt.....	24
Figure 23: Apparatus of hydrogen production used for GC.	25
Figure 24: Data from GC of hydrogen production using Mn ²⁺ doped ZnSe NPs with MPA, 7 nm ALD and 3 nm Pt for an hour.	26
Figure 25: Data from GC of hydrogen production using Mn ²⁺ doped ZnSe NPs with MPA, 7 nm ALD and 1 or 3 nm Pt through time.	27
Figure 26: Data from GC of hydrogen production using TiO ₂ through time.	28

ACKNOWLEDGEMENTS

Throughout the duration of this project, I received a lot of help and support from different people. First, I would like to express my deepest appreciation to John Asbury who is not only the research group conductor, but also the advisor for this project. His experience and intelligence helped solve many problems in the process of fulfilling this project, and his suggestion clearly direct this project. Also, his patience and gentleness greatly encourage me especially in hard times. It is my great pleasure to spend two-year undergrad in John's group. Second, I am extremely grateful to Kelsey Watson, a PhD candidate in John Asbury's group, who helped and gave a lot of guidance to this project. Since her PhD project related to the project I am doing, she taught me a lot about related information and gave very clear advice to this project. Also, many thanks to Bangzhi Liu for helping depositing Al_2O_3 layer and Pt layer onto the NPs. I would also to extend my gratitude to Rebecca Katz for helping conduct GC and give advice to this project.

Chapter 1

Information

Sub-Chapter 1: Background Information and Significance

With the huge energy consumption in the world in the past few decades, people will face the situation that no non-renewable resources, such as petroleum and coal, can be used in the near future. Nowadays, environmental damage and climate change show the significance of finding green and renewable energy resources. Therefore, the importance of sunlight has been brought great attention since the sun is a good renewable green energy resource. The concept of using solar energy to produce chemical energy, photocatalysis, has been a popular area of study these years. Photocatalytic reaction is a chemical reaction which absorbs light from sun to form excited electrons with nanoparticles (NPs) and photocatalysts.

Recently, people have started to study doped semiconductor nanoparticles in photocatalysis. Doping semiconductor NPs can modify the electronic, optical, biological, and magnetic properties of NPs. Previous work shows that the ligands that stabilize NPs can be oxidized by an excess accumulation of holes on the NP's surface, causing them to degrade during photocatalysis.³ The imbalance of electron and hole transfer rates,² resulting after photo-excitation, cause charges to accumulate on the NPs. This has been a major limitation for the NP photocatalysis field⁴ because electrons are easier to extract than holes.⁵ A buildup of electrons on the NP is generally not a problem since electrons can be easily extract from the NPs, while holes are harder to be extracted. Moreover, the NPs ligands are anionic and easy to be oxidized to form metallic

sites that can serve as beneficial catalytically active sites.⁶ However, the use of hole extracting ligands is not still good since the ligands limit the oxidation potential of the NPs⁷.

Thus, the long-excited state lifetime of Mn^{2+} doped NPs are desirable for photocatalysis because they enable electrons and holes to be available for catalytic reactions and balance the extraction of holes and the use of electrons in a reaction. Therefore, Mn^{2+} doped NPs can minimize the hole accumulation and the damage to oxidation.⁶ Thus, this thesis will focus on using Mn^{2+} doped NPs that have long excited state lifetimes in hopes of using these long lifetimes to overcome the imbalance of the electron and hole transfer rates.¹

Sub-Chapter 2: Research Plans

This project will take advantage of the remarkably long excited state lifetimes of Mn^{2+} doped NPs to overcome the imbalance of electron and hole transfer rates that has limited prior work in this field. The long-excited lifetime enables to better balance the hole and electrons transfer rate, which allows Mn^{2+} doped NPs to perform heterogenous or homogenous photocatalysis.

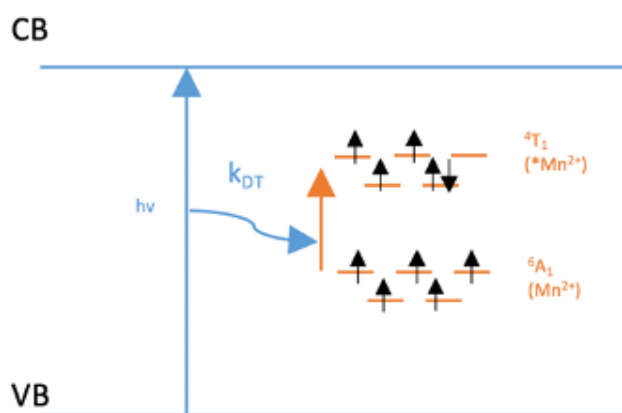


Figure 1: Electron configurations of ZnSe and Mn^{2+} doped ZnSe with spin-flip between 4T_1 and 6A_1 excited state.

Mn^{2+} doped ZnSe NPs are popular in this field because of the long-excited lifetime that have been reported up to $580 \mu\text{s}$ ⁸⁻¹⁰ and the fact that they are able to absorb visible light. The excited state lifetime of ZnSe NPs can be extended by eight orders of magnitude when doped with Mn^{2+} .¹¹ Once the Mn^{2+} doped ZnSe NPs are photoexcited, the electron transition between the 6A_1 ground state and 4T_1 excited state involves a spin-flip in the 4T_1 excited state, which has the higher energy as shown in Figure 1. This forbidden transition makes the excited state lifetime of ZnSe Mn^{2+} much longer. The long-excited state lifetime will allow these nanoparticles to be used in photocatalytic applications.

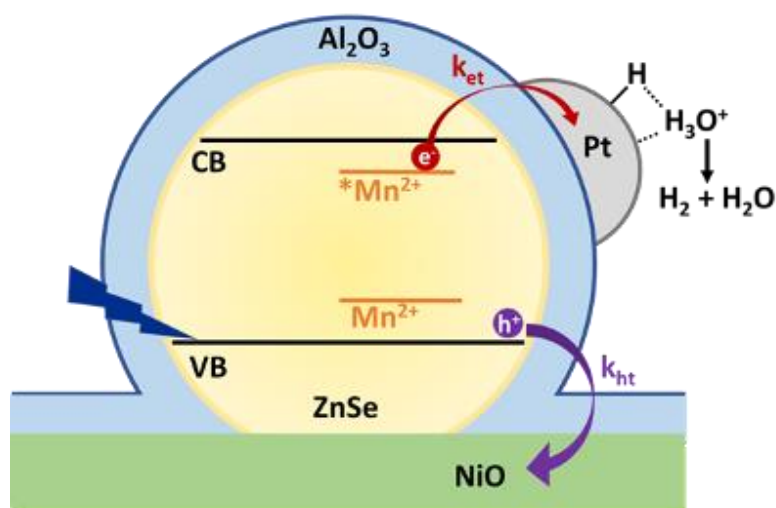


Figure 2: Architecture of photocatalytic Al₂O₃ coated ZnSe NPs doped with Mn²⁺ ions to be explored in this project.

Figure 2 illustrates the architecture of the Mn²⁺ doped ZnSe NPs that will be developed for this effort. This model consists of Mn²⁺ doped ZnSe NPs deposited onto a NiO electrode to enable transfer of holes to the NPs after photoexcitation. The electrodes with NPs will be overcoated with Al₂O₃ layers that will protect the NPs from chemical damage during catalysis and selectively slow electron transfer so it can be in balance with hole transfer. Al₂O₃ layer will be deposited by atomic layer deposition (ALD). Platinum particles will then be deposited by chemical vapor deposition (CVD) on the Al₂O₃ layer to enable the photoexcited electrons to be used to produce H₂ and demonstrate the stable and efficient photocatalytic system.

Chapter 2

Result and Discussion

Sub-Chapter 1: Synthesis Part

The synthesis procedure of ZnSe Mn²⁺ doped NPs was adapted and refined from several previous work by Kelsey, a Ph.D. candidate in John Asbury's group. With Kelsey's provided procedure, ZnSe Mn²⁺ doped NPs were made using a Schlenk line, as shown in Figure 3.

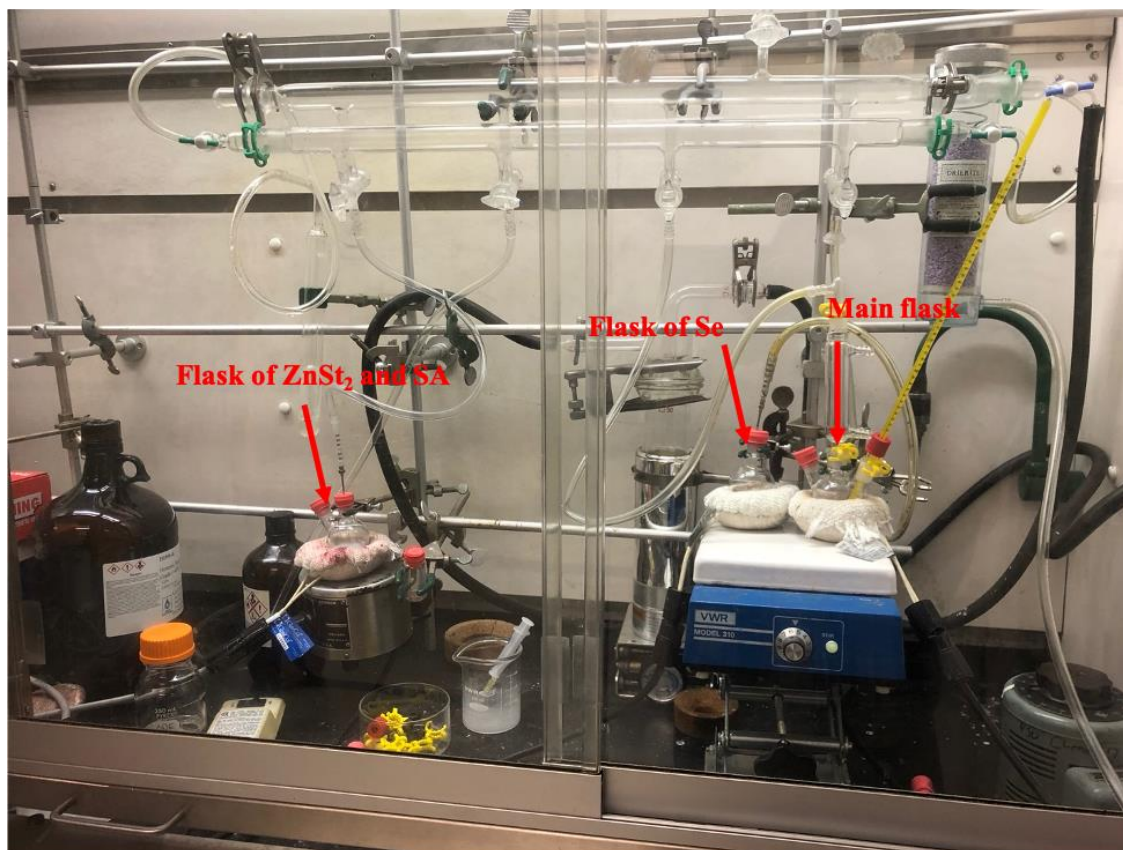


Figure 3: Apparatus of synthesis of Mn²⁺ doped ZnSe NPs.

In Figure 3, 0.002 mol of MnSt₂, 0.098 mol of ZnSt₂, and 5 mL of ODE were added to a 50 mL three-neck round flask (main flask), which was the left round flask, and degassed with N₂ at 110 °C for about 20 min. The main flask was heated to 290 °C for one minute with the

injection of Selenium (Se) powder. Then, the main flask was cooled to 250 °C for about ten minutes. Later, 1 mL of ZnSt₂ and SA precursor solution was added to the main flask twelve mins after the Se injection at 260 °C. The cooling process and injection of ZnSt₂ and SA precursor solution repeated three times. Last, the main flask was heated at 250 °C for another 40 minutes at constant N₂ flow. Then, the NPs were cooled to room temperature and purified by using methanol, hexane, and acetone. The Mn²⁺ doped NPs were synthesized with hot-injection synthesis method.

Then, after the purification, the emission of NPs was observed using a 374 nm UV lamp, as shown in Figure 4.

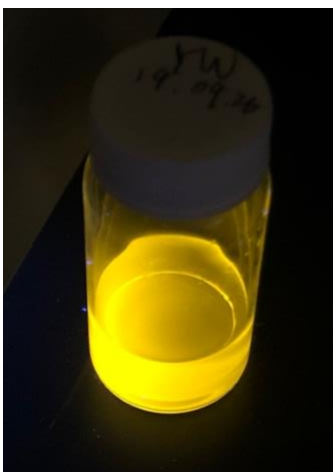


Figure 4: Fluorescence color of Mn²⁺ ZnSe NPs under the UV lamp (374 nm) made at Sept. 26, 2019.

Figure 4 shows the fluorescence of Mn²⁺ doped ZnSe NPs under 374 nm light using the provided synthesis procedure. The fluorescence of Mn²⁺ doped ZnSe NPs gives an easy prove of the NPs have been made. After the synthesis, emission, absorption, and PL were tested in order to make sure the Mn²⁺ doped ZnSe NPs made have the same electronic and optical properties. In previous work, ZnSe NPs will both absorb and emit light at 430 nm, while Mn doped NPs will

emit at 590 nm. From the data of absorption and emission, ZnSe Mn²⁺ has absorption at 430 and emission at 590 nm that are both shown in Figure 5 and 6.

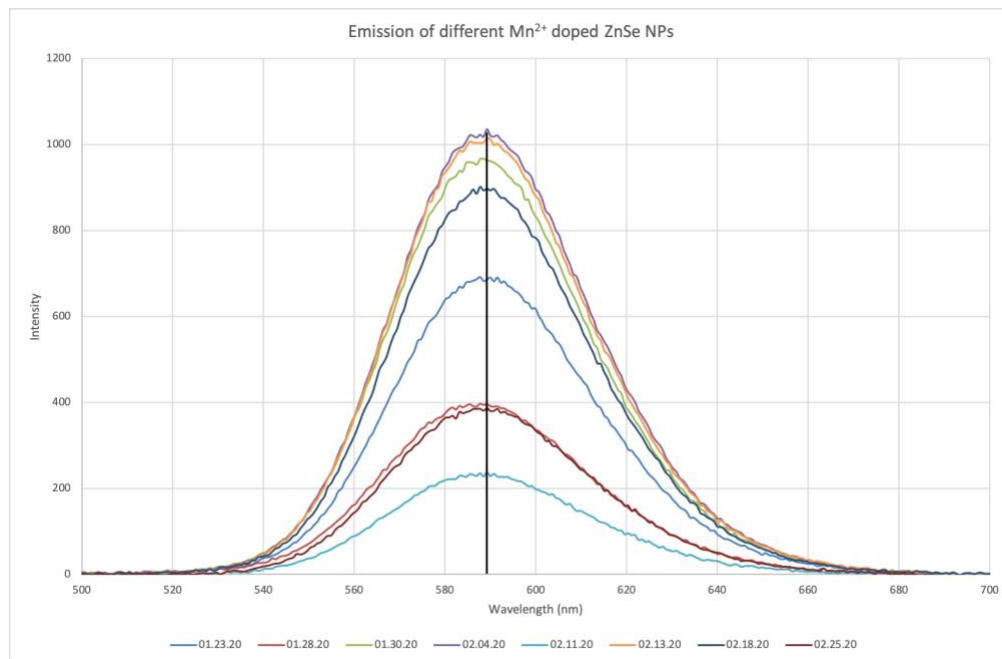


Figure 5: Emission data of eight samples of Mn²⁺ ZnSe NPs made at different dates.

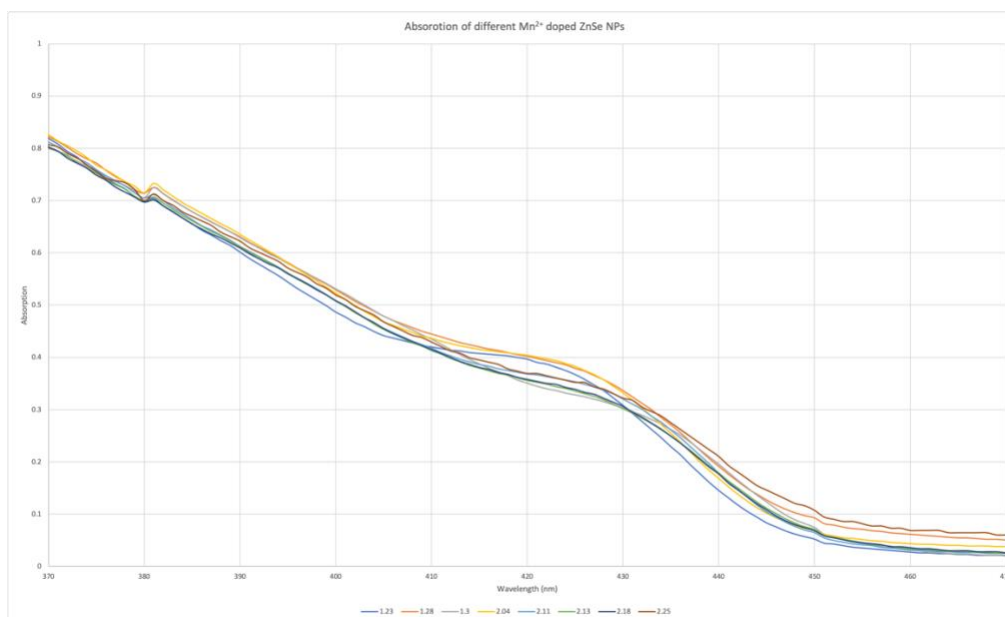


Figure 6: Absorption data of eight samples of Mn²⁺ ZnSe NPs made at different dates.

Figure 5 and Figure 6 are the results of eight samples made at different days in 2020. In Figure 5, the emissions of NPs were taken under 374 nm light and the intensity of each NPs was varied because of the different concentrations of NPs. In Figure 5, all NPs had the peak at 590 nm, which showed the NPs was doped with Mn. Figure 6 also showed the absorptions of eight samples from 350 nm to 470 nm. From Figure 6, the peak at 430 nm was found, which means ZnSe NPs had been made. Therefore, all these data together proved Mn²⁺ doped ZnSe NPs were made using the procedure. In addition, the consistency of all NPs shows the operability of the procedure. Moreover, the time-resolved photoluminescence (PL) spectroscopy was tested to prove the long-excited lifetime.

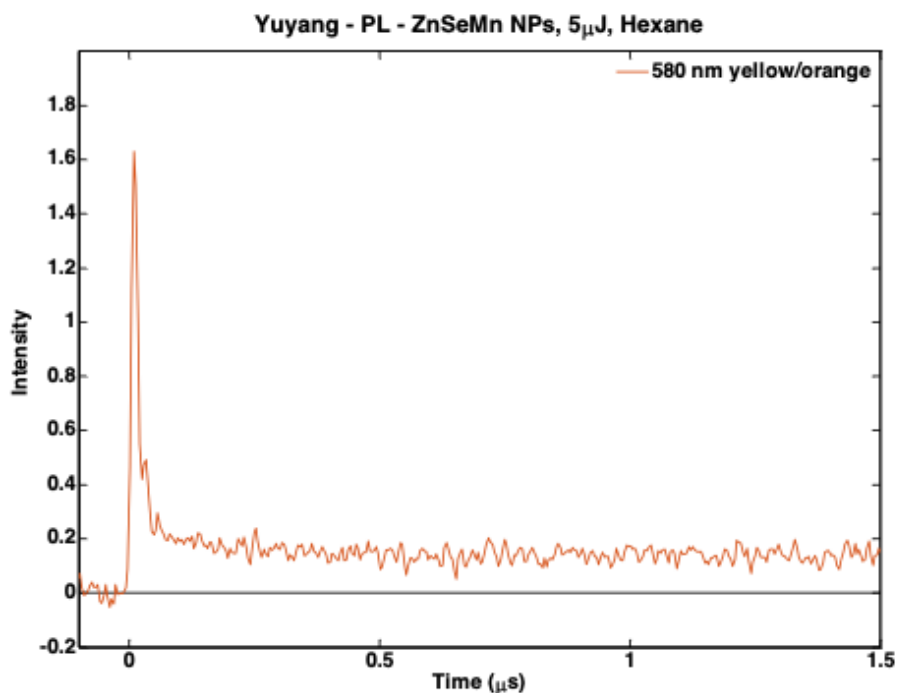


Figure 7: Time-resolved PL spectroscopy shows the long-excited state lifetime of Mn²⁺ doped ZnSe NPs.

Figure 7 shows the time-resolved PL spectroscopy of one sample in solution. The excited state lifetime is much longer than 1.5 μs even with low intensity, which indicates that Mn²⁺ ions

were successfully incorporated into the ZnSe NPs. Thus, from all the data tested and proved that using the provided procedure the Mn^{2+} doped ZnSe NPs can be consistently made.

Sub Chapter 2: Spin Coating NPs and Formatting the Structure

Different Mn^{2+} doped ZnSe NPs made at different time were mixed together if the absorption and emission data were the same as shown in Figure 5 and 6. Then, all Mn^{2+} doped ZnSe NPs were prepared and filtered with $1.0 \mu m$ PTFE filter to be deposited onto 5% (wt.) Al_2O_3 base films.

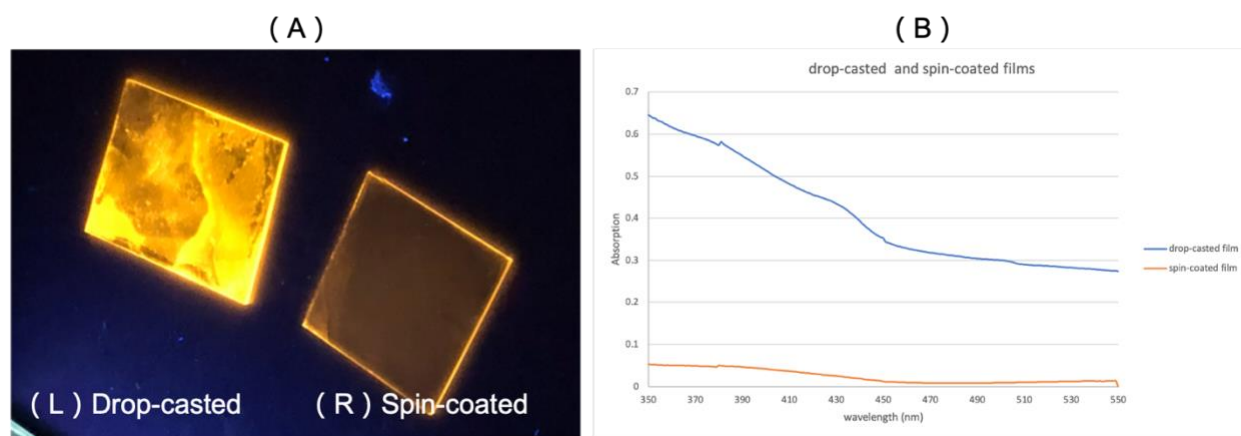


Figure 8: (A) Fluorescence of Mn^{2+} doped ZnSe NPs films using (L) drop-casted and (R) spin-coated method under the UV lamp. (B) Absorption data of two films.

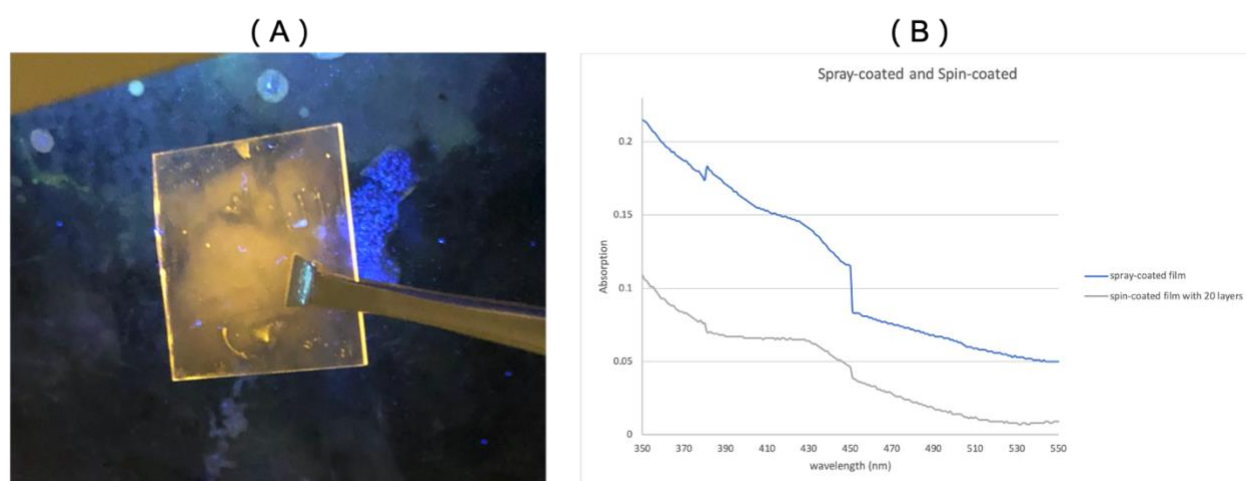


Figure 9: (A) Fluorescence of Mn^{2+} doped ZnSe NPs film using spray-coated method under the UV lamp. (B) Absorption data of spray-coated film and spin-coated film with 20 layers.

Figure 8 and 9 show the three different methods that used to deposit NPs on the films, which were drop-casting, spin-coating, and spray-coating. As shown in Figure 8 (A), the drop-casted film had brighter fluorescence under the UV lamp, but the film was not uniform, while the spin-coated film had a uniform layer. In Figure 8 (B), the absorption shows the difference between drop-casting and spin-coating method. Using the same NPs, the absorbance of drop-casted film was higher than the absorbance of spin-coated one. Thus, a higher absorption and more uniform film should be needed. Then, the spray-coated method was practiced to deposit NPs onto the film. In Figure 9 (A), the spray-coated film had a bright fluorescence and could build a uniform layer. As shown in Figure 9 (B), the absorption of spray-coated film and spin-coated film with 20 layers were measured and compared. Spin-coated film with 20 layers means the film was spin-coated with the same amount of NPs for 20 times using the same method. Then, from the absorption data in Figure 9 (R), the spin-coated film with 20 layers still had lower absorption than that of spray-coated film. Then, spray-coating method seemed to be the best choice. However, when spray-coated method was utilized, this method consumed a lot of NPs solution, which made the process not worth after all. Therefore, although drop-casting and spray-coating methods could give higher absorption data than the spin-coating method did, considering the uniform of the film, spin-coating method was used finally in the entire research.

In addition, 5% (wt.) Al_2O_3 base films were changed to 10% (wt.) Al_2O_3 base films because 10% (wt.) Al_2O_3 base films can stick more Mn^{2+} doped ZnSe NPs onto the film with a smaller number of layers. Moreover, since Mn^{2+} doped ZnSe NPs will be washed out the prior layer when deposited onto 10% (wt.) Al_2O_3 base films, the NPs were ligand exchanged with MPA in order to get higher absorption.

The next step is to test whether electrons can be transferred to an electron acceptor known as methyl viologen (MV^{2+}). This should quench the PL emission from the NPs but produce blue color from the transfer of the electrons to form MV^{1+} .



Figure 10: Fluorescence of Mn^{2+} doped ZnSe NPs with MPA under the UV lamp.

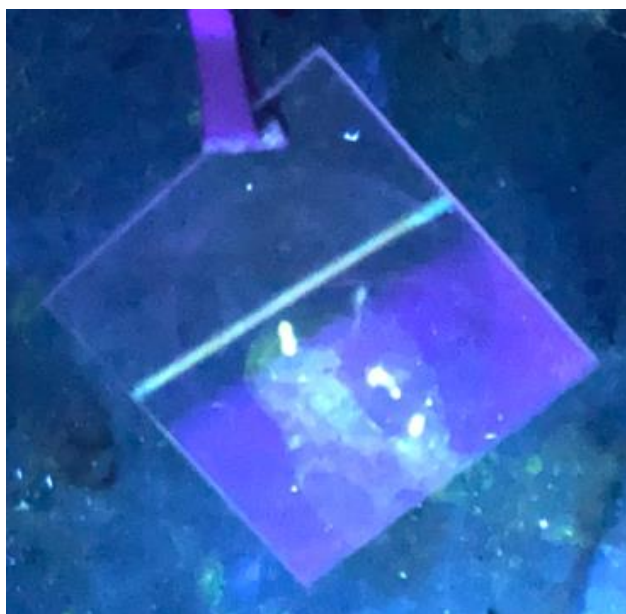


Figure 11: Fluorescence of Mn^{2+} doped ZnSe NPs with MPA and diheptyl MV^{2+} under the UV lamp.

Figure 10 and 11 show the fluorescence of Mn^{2+} doped ZnSe NPs with MPA film before and after reacted with 1,1'-Diheptyl-4,4'-bipyridinium dibromide, which is diheptyl MV^{2+} . In Figure 10, the film was still emitting under the UV lamp, while in Figure 11, the film was no longer emitting. Then, from the fluorescence, the NPs were either quenched by MV^{2+} or were washed out by MV^{2+} solution. Then, absorption was taken to prove the NP were not washed away but quenched.

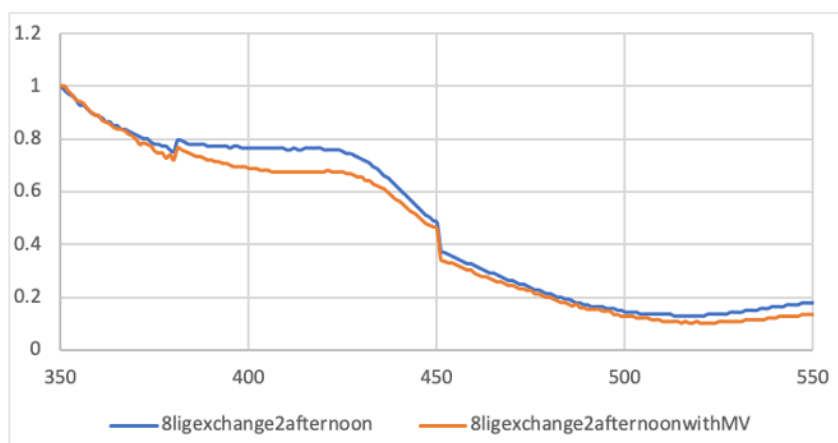


Figure 12: Normalized absorption data of 8-layer Mn^{2+} doped ZnSe NPs film with MPA before and after depositing diheptyl MV^{2+} .

Figure 12 shows the absorption data taken before and after adding MV^{2+} solution. In order to compare the data, both absorption data were normalized. Therefore, from Figure 12, the similar normalized absorption data of films shows that the NPs were still on the film after the addition of MV^{2+} solution, which means the Mn^{2+} doped ZnSe NPs film with MPA was quenched by diheptyl MV^{2+} instead of washing out.

Then, ultrafast transient absorption (TA) spectroscopy was taken to see the electron transferred from NPs to MV^{2+} . The film tested with absorption was tested again with TA spectroscopy.

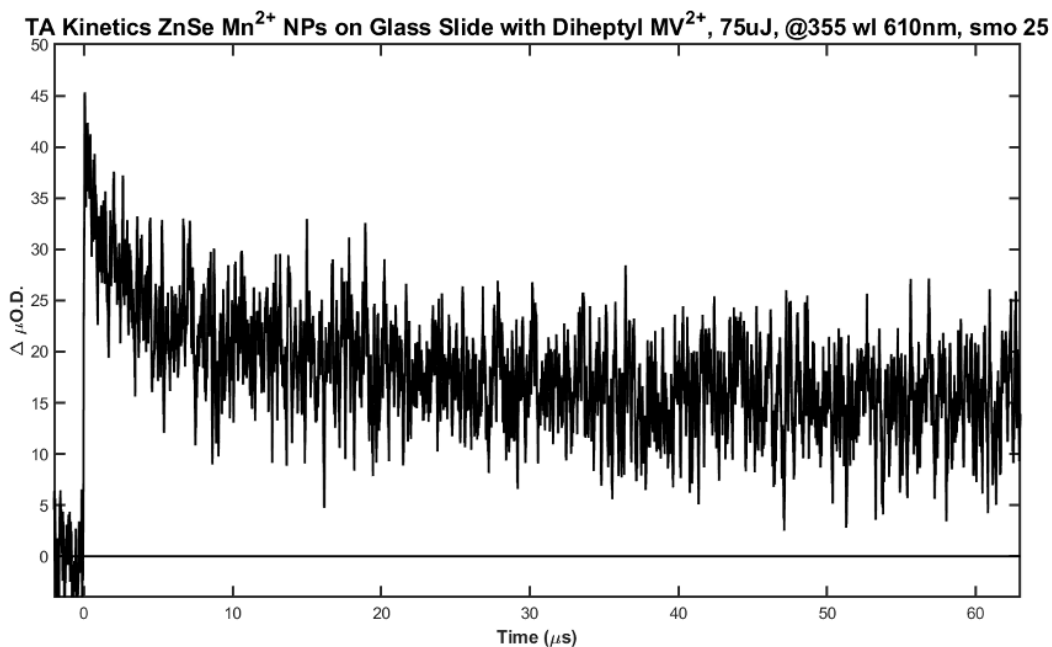


Figure 13: TA spectroscopy of Mn²⁺ doped ZnSe NPs film with MPA with diheptyl MV²⁺.

Figure 13 shows the TA spectroscopy for the film which was reacted with diheptyl MV²⁺. In reading the TA spectra, if a positive signal is observed in the spectra, this means that the electrons transfer from NPs to MV²⁺ to form MV¹⁺. Thus, in Figure 13, a clear signal was shown, electrons transferred from Mn²⁺ doped ZnSe NPs to MV²⁺ to form MV¹⁺. Then, electron transfer had been proved. The next step was to add Al₂O₃ as a protective layer, the Al₂O₃ layer would be deposited onto NPs layer, and then electron transfer through the Al₂O₃ layer needed to be proved. A protect layer is needed in the project since Mn²⁺ doped ZnSe NPs cannot stay in acidic environment, needed for hydrogen production. Then, with the Al₂O₃ layer, the Mn²⁺ doped ZnSe NPs films can stay longer in the acidic environment to produce hydrogen.

Atomic layer deposition (ALD) method was used in depositing another Al_2O_3 layer onto the Mn^{2+} doped ZnSe NPs with MPA layer to protect the NPs layer. Seven different samples were made and tested with PL spectroscopy before the Al_2O_3 deposition.

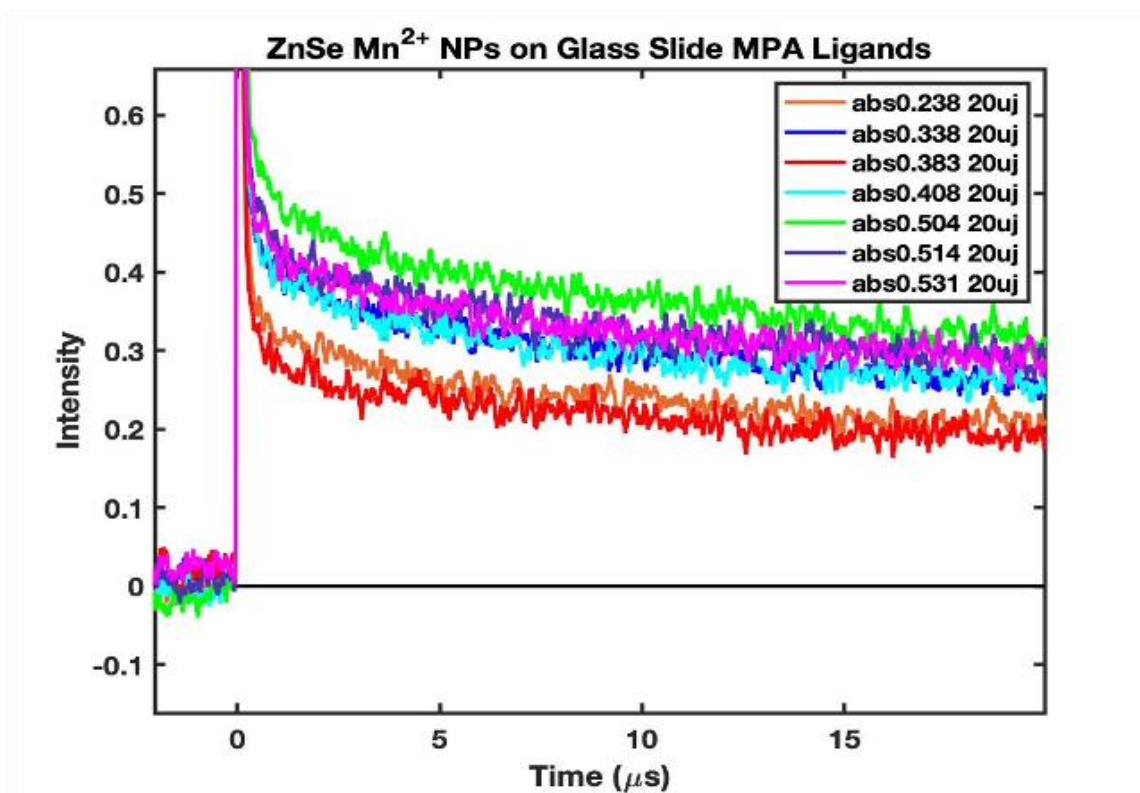


Figure 14: Time-resolved PL spectroscopy of seven Mn^{2+} doped ZnSe NPs films with MPA.

Figure 14 shows the PL spectroscopy of seven different samples, which each contained three layers of Mn^{2+} doped ZnSe NPs film with MPA. In Figure 14, all seven samples showed the long lifetime from PL spectroscopy. The PL spectroscopy of samples taken before adding Al_2O_3 layer used to compare the PL spectroscopy of samples taken after to find out the Al_2O_3 did not destroy the NPs layers. Then, four of seven samples were selected and added the Al_2O_3 protective layer for further test, which were sample 1 with abs. 0.383; sample 2 with abs. 0.514;

sample 3 with abs. 0.531; sample 4 with abs. 0.504. All four samples were added with different thickness of Al_2O_3 layer.

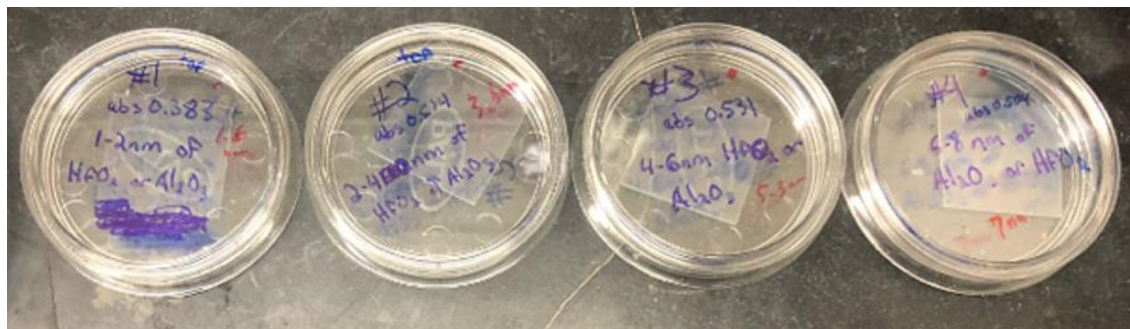


Figure 15: Four Mn^{2+} doped ZnSe NPs films with MPA with different thickness of Al_2O_3 layer.

Figure 15 shows the four sample with different thickness of Al_2O_3 layer, from which 1.6 nm of Al_2O_3 was added to sample 1 with abs. 0.383; 3.6 nm of Al_2O_3 was added to sample 2 with abs. 0.514; 5.3 nm of Al_2O_3 was added to sample 3 with abs. 0.531; 7.0 nm of Al_2O_3 was added to sample 4 with abs. 0.504. From Figure 15, no specific changes could be told from films, and the films were still transparent after adding protective Al_2O_3 layer.

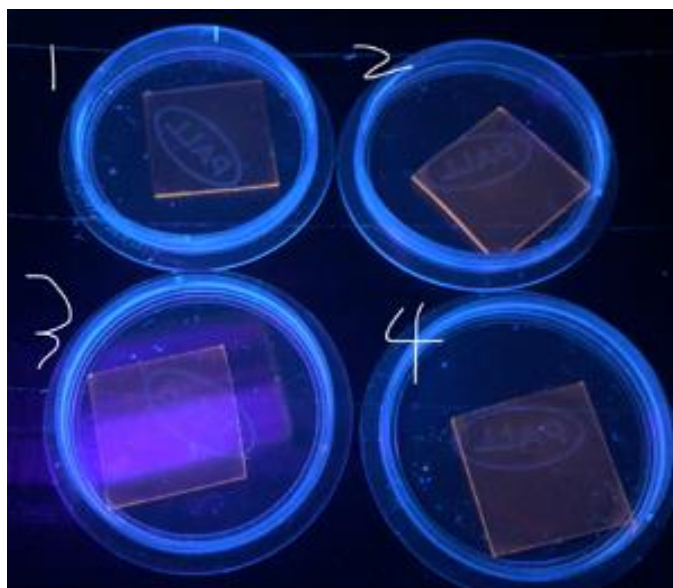


Figure 16: Fluorescence of four Mn^{2+} doped ZnSe NPs films with MPA with Al_2O_3 under the UV lamp.

Figure 16 shows the fluorescence of four samples with different thickness of protective Al_2O_3 layer under the UV lamp, in which all of them were emitting as normal films. Therefore, the Al_2O_3 layer did not destroy the film, and the absorption data of the four different samples were taken and shown below.

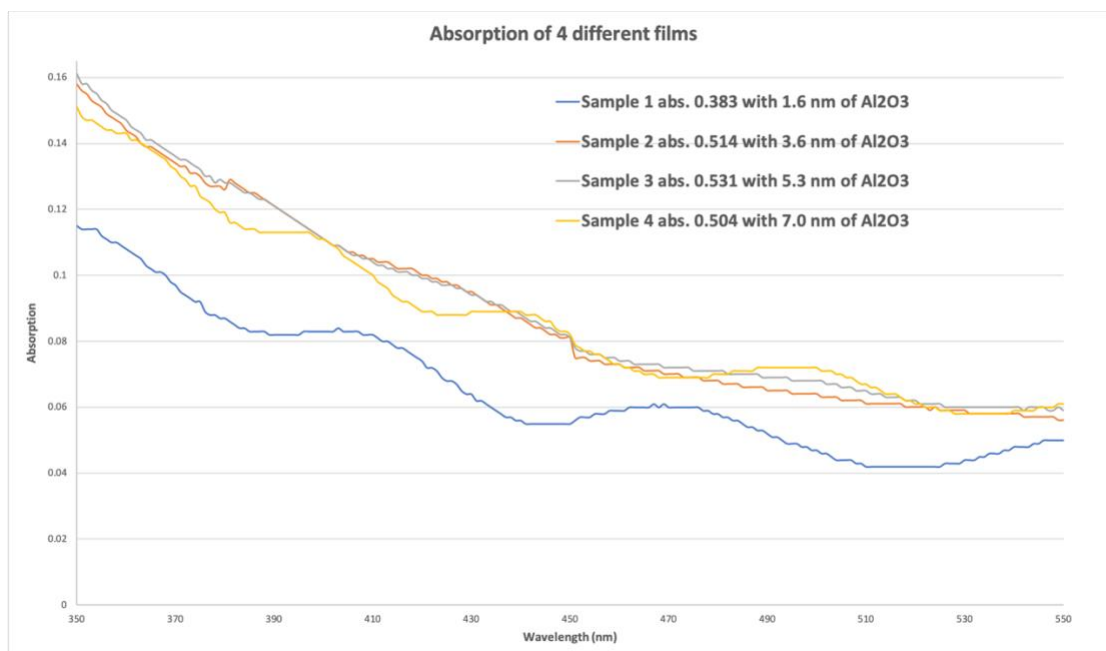


Figure 17: Absorption data of four Mn²⁺ doped ZnSe NPs films with MPA with different thickness of Al₂O₃ layer.

Figure 17 shows the absorption data for four samples with different thickness of Al₂O₃ layer. The absorption data were lower compared to taken before the deposition of Al₂O₃, but the absorption of four different films with different thickness of Al₂O₃ layer were still the same. Therefore, it is safe to use Al₂O₃ layer to protect NPs layer. Then, the PL spectroscopy was used to test the long lifetime of the NPs.

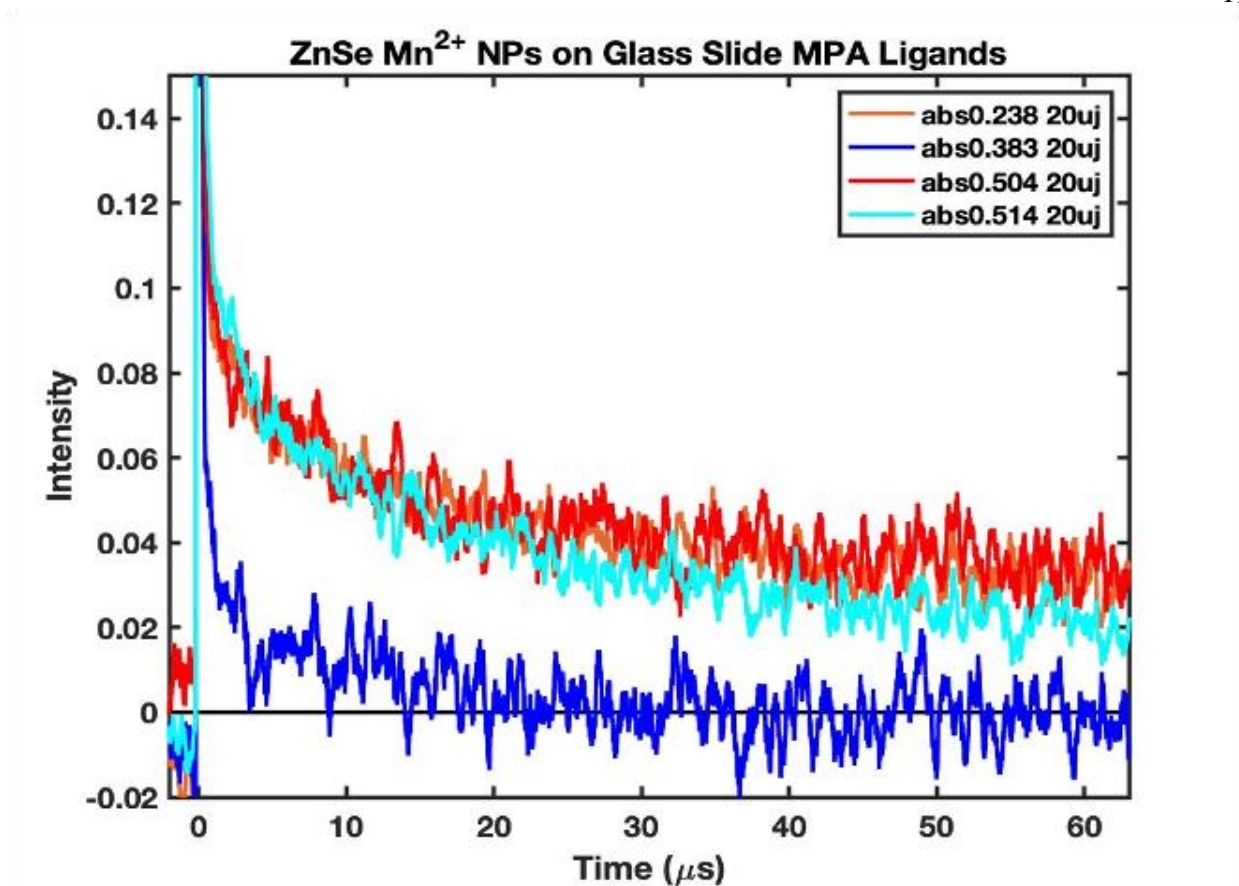


Figure 18: Time-resolved PL spectroscopy of four Mn²⁺ doped ZnSe NPs films with MPA with different thickness of Al₂O₃ layer.

Figure 18 shows the PL of four samples with different thickness of Al₂O₃ layer. In Figure 18, it still shows the long lifetime of Mn²⁺ doped ZnSe NPs. Therefore, the Mn²⁺ doped ZnSe NPs with MPA and Al₂O₃ films were safe to use in testing the electron transfer.

Then, the same steps were repeated with depositing MV²⁺ onto the films. Since diheptyl MV²⁺ solution in methanol destroyed the films, another MV²⁺ was used. MV²⁺ dichloride hydrate was used, which is soluble in water. Later, sample 2 abs. 0.514 with 3.6 nm of Al₂O₃ and sample 4 abs. 0.504 with 7.0 nm of Al₂O₃ were used to test with TA spectroscopy to see the electron transfer.

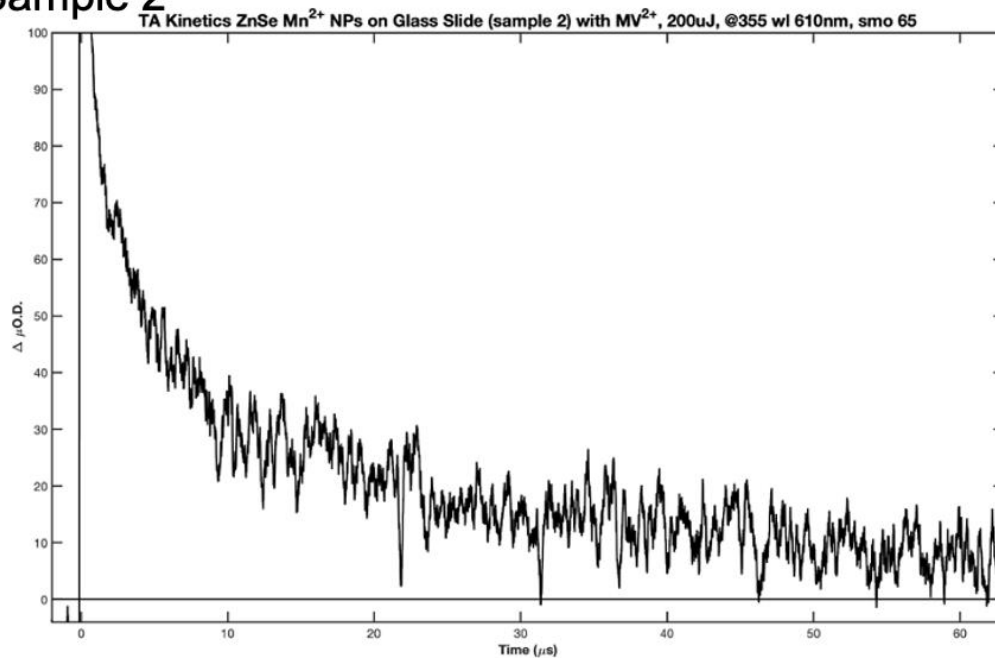
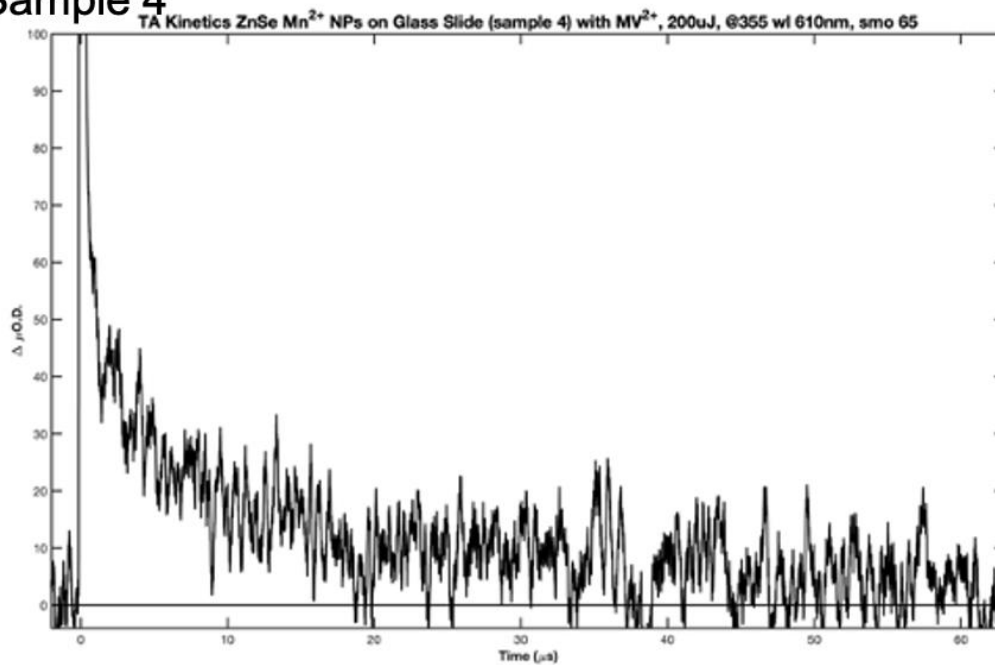
(A) Sample 2**(B) Sample 4**

Figure 19: TA spectroscopy of sample 2 and 4 with hydrate MV²⁺.

Figure 19 shows the two results of the TA spectroscopy for sample 2 and sample 4 with hydrate MV^{2+} . Sample 2 had a bigger signal than sample 4 did, since sample 2 had thinner layer than sample 4 did. Thus, in both of the samples, a signal of electron transfer found using TA spectroscopy, which means the electrons could transfer the Al_2O_3 layer as thick as 7 nm. Therefore, in the further research, the thickness of Al_2O_3 layer was set to be 7 nm.

Chapter 3

Future Work

In chapter 2, the thickness of Al_2O_3 layer was decided to be 7 nm, and the electron transfer through Al_2O_3 from NPs was proved. Thus, the next step was to deposit Platinum (Pt) layer onto the film and produce hydrogen using the Mn^{2+} doped ZnSe NPs film. In previous work, ascorbic acid (AA, 0.1 to 1.0 M) in 50:50 ethanol: water was used to produce hydrogen.¹² Ascorbic acid was used as the potential source of hydrogen and a buffer solution to maintain the pH even as the protons were reduced to hydrogen. Therefore, 0.5 M of AA in 50:50 ethanol: water was used in the following experiment. Then, a test of the thickness of Pt was needed. Four Mn^{2+} doped ZnSe NPs films with similar absorption were prepared to be deposited with 7 nm of Al_2O_3 and different thickness (1-7 nm) of Pt.

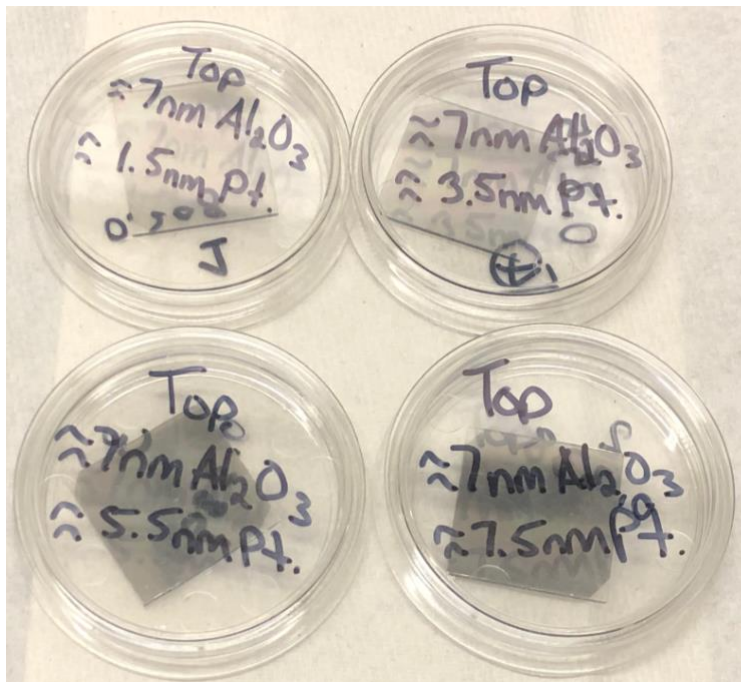


Figure 20: Four Mn^{2+} doped ZnSe NPs films with MPA and 7 nm Al_2O_3 with different thickness of Pt layer.

Figure 20 shows four Mn^{2+} doped ZnSe NPs samples with different thickness of Pt layer, which are sample 1 with 1.5 nm Pt; sample 2 with 3.5 nm Pt; sample 3 with 5.5 nm Pt; sample 4 with 7.5 nm Pt. From Figure 20, the film with thicker layer of Pt as sample 4 had darker outlook than the film with thinner layer as sample 1. Then, the fluorescence of these four films was taken to see the change of each film.

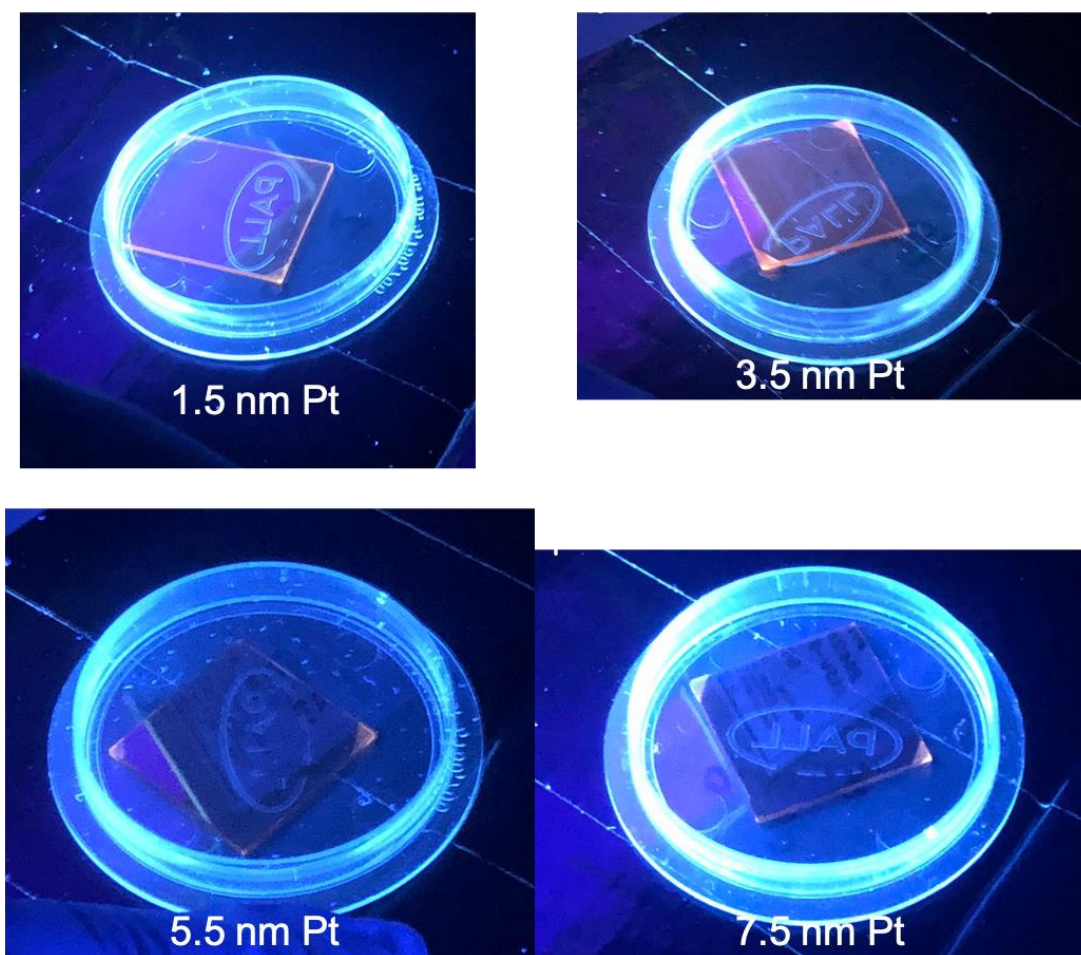


Figure 21: Fluorescence of four Mn^{2+} doped ZnSe NPs films with MPA and 7 nm Al_2O_3 with different thickness of Pt under the UV lamp.

In Figure 21, the fluorescence of four samples were taken. From the fluorescence, the films (sample 3 and sample 4) with thicker Pt layer were no longer emitting, as the films (sample 1 and

sample 2) with thinner Pt layer were still emitting. The Mn^{2+} doped ZnSe NPs films with Pt layer should not be emitting since Pt will quench the NPs. Thus, the Mn^{2+} doped ZnSe NPs films with thinner Pt layer were still emitting since the Pt layer could only quench the top layer of NPs as the thicker Pt layer could quench the whole layer of NPs.

Then, a raw test took place to see whether the Mn^{2+} doped ZnSe NPs film with Pt layer could produce hydrogen in acidic environment under the UV light which had enough energy to excite the electrons to produce hydrogen. The film with 1.5 nm Pt (sample 1) was placed in the shelf to set straight in front of the light and put inside the 0.5 M AA in 50:50 ethanol: water solution as shown below.



Figure 22: Mn^{2+} doped ZnSe NPs with MPA and 7 nm ALD and 1.5 nm Pt in Ascorbic Acid under the UV lamp for 30 min.

In Figure 22, sample 1 was excited under the UV lamp for 30 mins, and small bubbles were found formed on the film. No bubbles were found before the reaction started. And the small bubbles were found to be gas bubbles, but no conclusions can be made to prove that the small gas bubbles were hydrogen. Then, more accurate experiments should be taken.

Then, the further experiment was done using gas chromatography (GC), which could tell the exact concentration of hydrogen production. In addition, the same experiment was done with film with the thickest Pt layer, which is 7.5 nm. However, after one hour, no bubbles were found formed under the UV light. Then, another thought was brought up: the thickness of Pt would affect the production of hydrogen. With thicker Pt layer, less hydrogen will be produced and longer time will be needed to produce the same amount of hydrogen. Thus, in the further experiment, only 1 nm, 2 nm, and 3 nm of Pt layer on Mn^{2+} doped ZnSe NPs film was tested for hydrogen production.

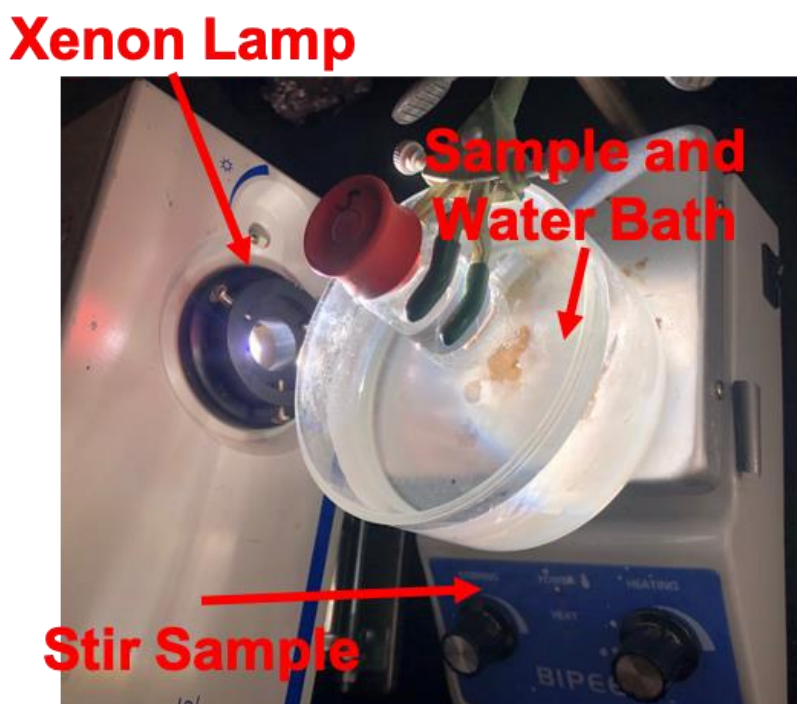


Figure 23: Apparatus of hydrogen production used for GC.

Figure 23 shows the apparatus used for hydrogen production. The vial and the rubber cap were used for air tightness, which was checked to be no leak for at least 24 hours. In addition, in order to put the film inside the vial, a smaller film was made. The xenon lamp was used to excite electrons to transfer to form hydrogen. The water bath was needed since the xenon lamp heated the sample and the water bath would keep the sample cool. Before testing, the vial was degassed with nitrogen for 15 mins to get rid of any air in the vial. In the later experiment, the efficiency of using N₂ to degas was not good, since oxygen would still stay inside. Argon was used in further experiment. Also, the head space of the vial was calculated using gravimetric method, which was 7.9 ± 0.1 mL.

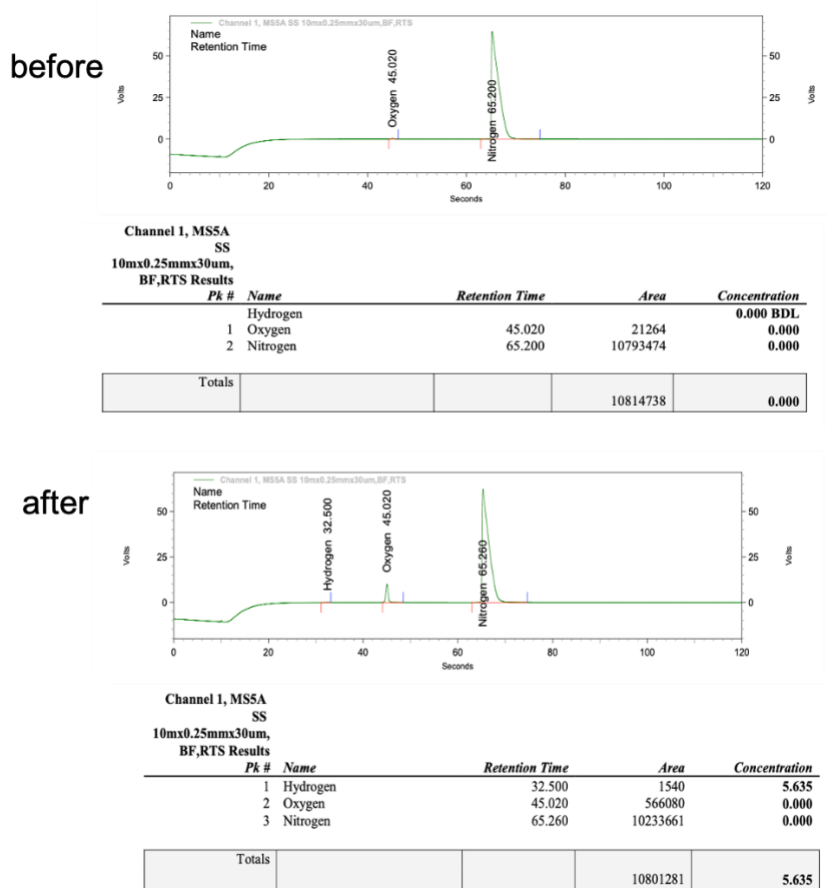


Figure 24: Data from GC of hydrogen production using Mn²⁺ doped ZnSe NPs with MPA, 7 nm ALD and 3 nm Pt for an hour.

Figure 24 shows the hydrogen production using NPs film with 3 nm Pt layer in an hour. The Mn^{2+} doped ZnSe NPs film with 3 nm Pt was put in the apparatus shown in Figure 23. In this experiment, the vial was first degassed with N_2 for 15 mins, and then excited with xenon lamp for an hour. Two tests were taken for measuring the H_2 production. In Figure 24, the upper part shows no hydrogen was in the vial before exciting with xenon lamp, while the lower part shows after one hour, 5.635 ppm of H_2 was made in the vial, which was 0.0018 μmol of H_2 . In addition, the GC was set up to not to calculate the concentration of oxygen and nitrogen. Therefore, with the NPs film with 3nm Pt layer in AA solution, hydrogen gas was made with electron transfer. Then, more tests were made. Moreover, all NPs with Pt layer were able to produce H_2 under the same condition. Thus, NPs films with 1 nm and 3 nm Pt layer were tested under the same condition for about 24 hours. Several data were taken.

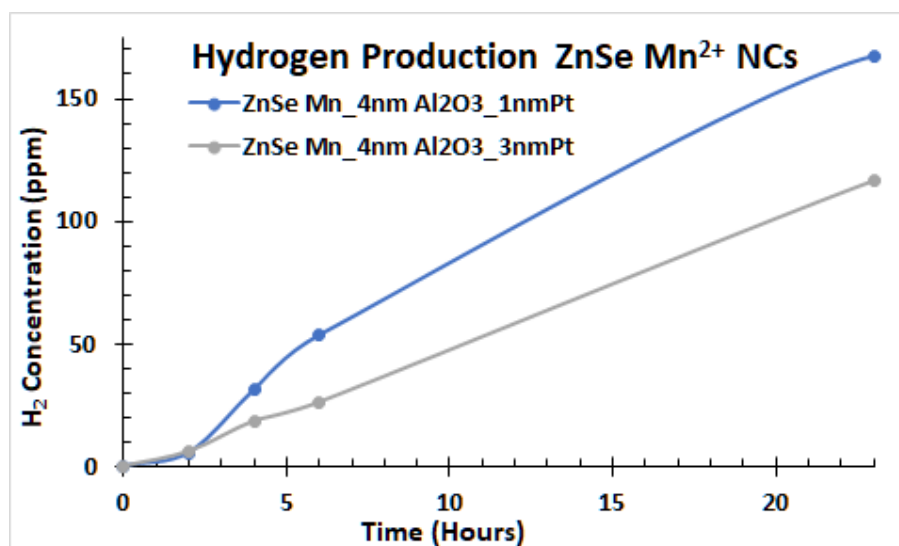


Figure 25: Data from GC of hydrogen production using Mn^{2+} doped ZnSe NPs with MPA, 7 nm ALD and 1 or 3 nm Pt through time.

Figure 25 shows the concentration of H_2 produced in the vial over 23 hours. The NPs film with 1nm Pt layer and the NPs film with 3 nm Pt layer were tested separately. As shown in

Figure 25, more H₂ was produced with NPs film with 1 nm Pt layer than the film with 3 nm Pt layer under the same condition as shown in Figure 23. Therefore, it proved the thought that the thicker layer of Pt will have less H₂ produced. However, more experiments should be conducted to prove this thought further. Moreover, the maximum production of hydrogen was up to 167 ppm (or 0.0539 μmol) in the vial for NPs film with 1 nm Pt layer, while the maximum production of hydrogen was up to 117 ppm (0.0378 μmol) in the vial for NPs film with 3 nm Pt layer. Also, the H₂ production kept increasing over time. Thus, for the future study of the hydrogen production with Mn²⁺ doped ZnSe NPs, more experiments should be done with 1 nm Pt layer to test the production. Also, Mn²⁺ doped ZnSe NPs was compared with TiO₂, which is a good catalyst to use in photocatalysis. TiO₂ was used widely in electrocatalysis as a standard.

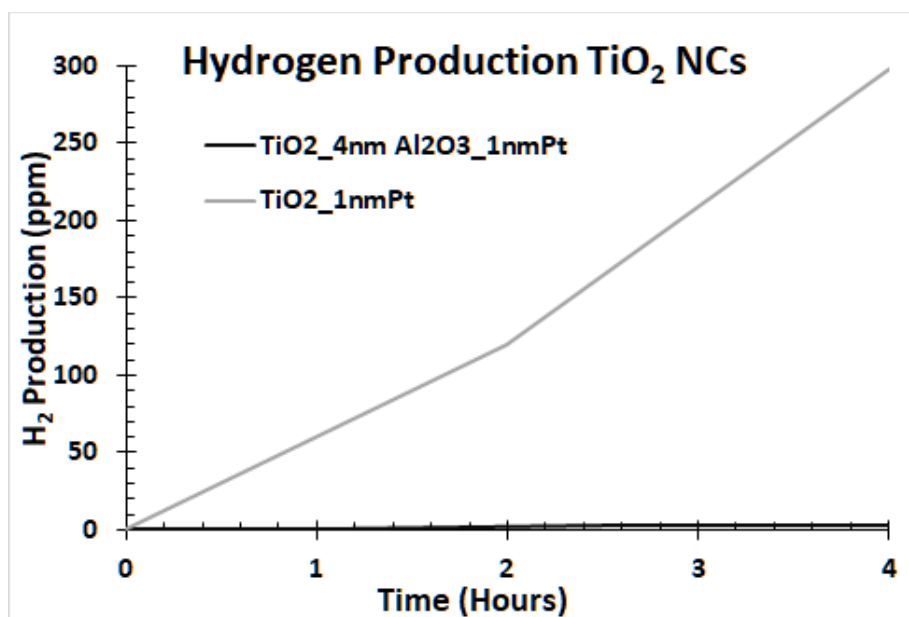


Figure 26: Data from GC of hydrogen production using TiO₂ through time.

Figure 26 shows the hydrogen production using two different films with TiO₂. One film was spin-coated with TiO₂ and had 4 nm Al₂O₃ layer and 1 nm Pt layer on, while the other one

was spin-coated with TiO₂ and only 1 nm Pt layer. Therefore, with only 1 nm Pt, hydrogen produced up to 300 ppm in 4 hours. Compared to the production with NPs film with 1 nm Pts in Figure 25, TiO₂ produced more hydrogen. Therefore, for future study, the efficiency of hydrogen production with Mn²⁺ doped ZnSe NPs should be studied.

At last, the final step of the study was to deposit the whole structure done before onto the NiO layer as shown in Figure 2. Then, the experiment for hydrogen production will be tested again to find out whether hydrogen gas will be produced. Moreover, the efficiency of the structure shown in Figure 2 using Mn²⁺ doped ZnSe NPs will be measured.

BIBLIOGRAPHY

1. Khaparde, R.; Acharya, S., Effect of isovalent dopants on photodegradation ability of ZnS nanoparticles. *Spectrochim Acta A Mol Biomol Spectrosc* 2016, 163, 49-57.
2. S. Logunov, T.G., S. Marguet, and M. A. El-Sayed (1998). Interfacial Carriers Dynamics of CdS Nanoparticles. *J. Phys. Chem. A* 102, 5652–5658.
3. Kamat, P.V., Christians, J.A., and Radich, J.G. (2014). Quantum dot solar cells: hole transfer as a limiting factor in boosting the photoconversion efficiency. *Langmuir* 30, 5716-5725.
4. Wu, K., Chen, Z., Lv, H., Zhu, H., Hill, C.L., and Lian, T. (2014). Hole removal rate limits photodriven H₂ generation efficiency in CdS-Pt and CdSe/CdS-Pt semiconductor nanorod-metal tip heterostructures. *J Am Chem Soc* 136, 7708-7716.
5. S. Logunov, T. G., S. Marguet, and M. A. El-Sayed, Interfacial Carriers Dynamics of CdS Nanoparticles. *J. Phys. Chem. A* 1998, 102 (28), 5652–5658.
6. Kodaimati, M. S.; McClelland, K. P.; He, C.; Lian, S.; Jiang, Y.; Zhang, Z.; Weiss, E. A., Viewpoint: Challenges in Colloidal Photocatalysis and Some Strategies for Addressing Them. *Inorg Chem* 2018, 57 (7), 3659-3670.
7. Lian, S.; Weinberg, D. J.; Harris, R. D.; Kodaimati, M. S.; Weiss, E. A., Subpicosecond Photoinduced Hole Transfer from a CdS Quantum Dot to a Molecular Acceptor Bound Through an Exciton-Delocalizing Ligand. *ACS Nano* 2016, 10 (6), 6372-82.
8. Pu, C.; Ma, J.; Qin, H.; Yan, M.; Fu, T.; Niu, Y.; Yang, X.; Huang, Y.; Zhao, F.; Peng, X., Doped Semiconductor-Nanocrystal Emitters with Optimal Photoluminescence Decay Dynamics in Microsecond to Millisecond Range: Synthesis and Applications. *ACS Cent Sci* 2016, 2 (1), 32-9.

9. Pradhan, N.; Das Adhikari, S.; Nag, A.; Sarma, D. D., Luminescence, Plasmonic, and Magnetic Properties of Doped Semiconductor Nanocrystals. *Angew Chem Int Ed Engl* 2017, 56 (25), 7038-7054.
10. Sarma, N. P. a. D. D., Advances in Light-Emitting Doped Semiconductor Nanocrystals. *J. Phys. Chem. Lett.* 2011, 2 (21), 2818–2826.
11. Pradhan, N.; Das Adhikari, S.; Nag, A.; Sarma, D. D., Luminescence, Plasmonic, and Magnetic Properties of Doped Semiconductor Nanocrystals. *Angew Chem Int Ed Engl* 2017, 56 (25), 7038-7054.
12. Han, Z., Qiu, F., Eisenberg, R., Holland, P. L., & Krauss, T. D. (2012). Robust photogeneration of h₂ in water using semiconductor nanocrystals and a nickel catalyst. *Science*, 338(6112), 1321-1324. doi:10.1126/science.1227775

ACADEMIC VITA

Working Experience

Undergraduate Researcher, The Pennsylvania State University, University Park, PA

John Asbury's Research Group

Aug 2019 - May 2021

- Synthesized and analyzed ZnSe Mn nanoparticles (NPs).
- Spin coated ZnSe Mn nanoparticle films onto Al₂O₃ base.
- Performed solid state ligand exchange of ZnSe Mn NPs from native stearate ligands to MPA ligands.
- Tested the absorption and emission of both ZnSe Mn solutions and films.
- Used transient absorption (TA) spectroscopy to observe electron transfer in ZnSe Mn solutions and films.
- Used steady state and time resolved photoluminescence (PL and TRPL) spectroscopy to quantify the excited state lifetime for lifetime of both ZnSe Mn solutions and films.

Learning Assistant (LA), The Pennsylvania State University, University Park, PA

LA for Quantum Chemistry

Spring 2021

- Due to my excellent performance in Quantum Chemistry, I was selected as a LA for the Spring 2021 course.
- Helped to facilitate collaborative active learning exercises, both during class and during problem-solving sessions outside of class

Junior Organic Chemist, Viva Biotech (Shanghai) Ltd, Shanghai, China

Gengjie Xu's Program Group

May 2019 - July 2019

- Collected data and analyzed the progress of each team member.
- Synthesized and purified a target compound.
- Used rotary evaporator to concentrate, dry, and separate target sample.
- Used liquid chromatography-mass spectrometry (LC-MS) and nuclear magnetic resonance (NMR) to determine the target products.

Peer Tutor, Pennsylvania State York, York, PA

Learning center

Aug 2018 - May 2019

- Tutored General Chemistry, Calculus, and Toefl students.
- Tutored up to six students each week.

Awards:

- Dean's list Aug 2017 – May 2020
- Erickson Discovery Grant Jun 2020
- The Joseph A. Dixon Memorial Scholarship in Chemistry Aug 2020 – May 2021